# Temperature dependence of elastic moduli of polycrystalline β plutonium

Yoko Suzuki, V. R. Fanelli, J. B. Betts, F. J. Freibert, C. H. Mielke, J. N. Mitchell, M. Ramos, T. A. Saleh, and A. Migliori

# Temperature dependence of elastic moduli of polycrystalline beta plutonium

Yoko Suzuki [a)], V. R. Fanelli, J. B. Betts, F. J. Freibert, C. H. Mielke, J. N. Mitchell, M. Ramos, T. A. Saleh and A. Migliori

*National High Magnetic Field Laboratory and Nuclear Materials Science Group, Los Alamos National Laboratory, Los Alamos, NM 87545, USA*

The elastic moduli of pure polycrystalline beta plutonium were measured over its full range of existence (417 K to 491 K) using resonant ultrasound spectroscopy. The Debye temperature (138 K), Poisson's ratio (0.28), Grüneisen parameter (2.3), and the zero-temperature atomic volume (21.2 $\text{Å}^3$) were computed from the measurements. Both bulk and shear moduli decrease smoothly on warming with expected discontinuities at the phase boundaries. The shear modulus is surprisingly nearly the same for beta and gamma Pu. The temperature dependence of bulk moduli for beta Pu is, like gamma Pu, unusually small. Poisson's ratio shows very strong differences among alpha, beta, and gamma Pu indicating they are entirely different metals. The zero-temperature elastic moduli were computed for the three phases as well as for gallium-stabilized delta Pu (also measured by us) and compared to calculations.

[a)] Author to whom correspondence should be addressed. Electronic mail: yoko@lanl.gov

## I. INTRODUCTION

Plutonium is one of the two most interesting elements because it has six crystallographic allotropes, unusual thermal expansion, and apparently completely different bonding behavior among its phases.[1] Some of its isotopes can sustain a fission chain reaction.[2] Surprisingly, neither accurate elastic moduli measurements exist, nor do satisfactory first-

principles electronic structure models; the first because of the difficulties in working with Pu,[3-6] the second because Pu electrons straddle the itinerant/localized boundary, frustrating understanding.[7-11] Lacking essential measurements for a very challenging element further distances understanding.

The lowest-temperature ($\alpha$) phase (Fig. 1) of Pu crystallizes in a low symmetry monoclinic structure, unusual for any metal, with a 16-atom unit cell.[12] At 398 K, the volume expands by 10% and forms a body-centered monoclinic structure with a perhaps 34-atom unit cell ($\beta$) phase.[13] At 488 K, the volume expands by 3% and forms a face-centered orthorhombic structure with an 8-atom unit cell ($\gamma$) phase.[14] At 593 K, the volume expands by 7% (25% larger than that of the alpha phase) and forms the (close-packed) face-centered cubic ($\delta$) phase with the largest solid volume and negative thermal expansion.[15] The volume contracts at 736 K for the $\delta$' phase with dubious properties,[16] followed by the ($\epsilon$) body-centered cubic structure at 756 K[15] until it liquefies at 913 K.[17] This complex phase diagram occurs within a factor of two in absolute temperature,[18] indicating how delicate the energy and entropy balances must be.

One set of properties that are incompletely measured[19-23] are the adiabatic elastic moduli, the second derivatives of energy respect to strains, and often the first properties computed from the many electronic structure models.[24-38] Elastic moduli are also one of a few thermodynamic susceptibilities which are essential for an understanding of the phases of Pu[39-49], and with their temperature dependence are important for applications.

For these reasons, Young's modulus and shear modulus were measured by several investigators. In 1960 by a resonance method for all six phases,[50, 51] Pu was thermally cycled many times. After each cycle, the moduli changed.[50] The most reliable bulk

modulus measurements were by Linford and Kay[52] (Fig. 2). Young's modulus was also measured by an extensometer for four phases[53] and by an ultrasonic resonance method for six phases[54]. There are many elastic modulus measurements at room temperature for α-Pu[55-58]. Temperature dependence of α-Pu moduli over a limited temperature range was measured by an ultrasonic resonance method[59-61], by an ultrasonic pulse technique[62] and by non-contacting laser-ultrasonics[63]. The β–α transformation was studied with an ultrasonic pulse technique.[64] The relative shear modulus as well as ultrasonic attenuation were measured using an inverted torsion pendulum for the six phases.[65] All pure Pu measurements were performed with polycrystalline samples because monocrystalline pure Pu was not available, however monocrystalline elastic moduli were measured in gallium-stabilized δ-Pu (δ-Pu 3.3 at. % Ga) at ambient temperature using a pulse-echo method by Ledbetter and Moment.[66] Inelastic x-ray scattering measurement produced values close to the Ledbetter and Moment result.[67] The temperature dependence of elastic moduli for polycrystalline δ-PuGa was measured by non-contacting laser-ultrasonics[63], by a high-pressure x-ray measurement[68] and by resonant ultrasound spectroscopy (RUS) for different gallium concentrations[69]. δ-PuAl was also measured by an ultrasonic resonance method[61] and RUS.[43] The change of elastic moduli with time was used to study Pu aging by self-irradiation in α-Pu and δ-PuGa.[70]

## II. MEASUREMENTS

Resonant ultrasound spectroscopy (RUS)[71-73] measurements of the adiabatic bulk and shear moduli of pure polycrystal β-Pu are reported here. The Pu measured had the highest available purity, and measurements were completed without thermal cycling. One

specimen was used for the work described here on the β phase. It was also used for measurement of α–Pu above 300 K, and γ–Pu. The specimen was made from electro-refined [239]Pu with 99.96 wt % Pu, 115 ppm W, 49 ppm Np, 50 ppm O, 53 ppm Si, 32 ppm Am and the sum of remaining impurities less than 25 ppm. The specimen was cut from a larger button that was arc melted and quenched to room temperature on a copper hearth, cut and polished, examined optically for voids and metallurgical defects, and the process repeated (about 10 times) until metallurgical imperfections were judged negligible.[20]

By usual metallographic cut-grind-polish method, the specimen was prepared in a parallelepiped of 0.265 x 0.268 x 0.270 cm$^3$ all ±0.002 cm. The immersion density at 300 K was determined to be 19.55 g/cm$^3$ ±0.02%. The density determined from mass and dimensions at 300 K is 19.70 g/cm$^3$ and the x-ray diffraction density is 19.86 g/cm$^3$ at 294 K. While the differences are small, thermal activation of defects makes it impossible to achieve (and unreasonable to expect) x-ray density in Pu above cryogenic temperatures.

Temperature was controlled by a helium gas-flow cryostat. Measurements were made in (constantly pumped) vacuum. The specimen was heated only once (after sample preparation where it was hearth-quenched) from room temperature to 650 K by approximately 2 K per hour. A crude dilatometer recorded length jumps at the same temperatures at which the elastic moduli displayed step-like changes at the phase transitions.

The technique used for the measurements, RUS, acquired resonance frequencies that were very different for different phases, while the variation for frequencies within

phases was smooth.[74] The typical resonances and the detailed descriptions for the RUS fit

process for α-Pu[19, 20], γ-Pu[21] and δ-Pu 2.36 at. % Ga [22, 23] are described elsewhere.

For the specimen of β-Pu (see Fig. 3) used here, the frequency was swept

typically from 0.2 to 1 MHz.[75] The inverse calculation (RUS fit)[76] was used to obtain two

polycrystalline elastic moduli, $C_L$ (the longitudinal sound speed is controlled by this

modulus) and the shear modulus, $G$ where the bulk modulus can be calculated by $B=C_L-$

$(4G/3)$. Errors arise principally from errors in sample geometry and the measurement of

dimensions. The recorded resonances have relatively low Q (typically 400-700) with

many resonances overlapped with each other. The resonances that appeared as shoulders

of larger resonances or had large background noise were omitted from the fit. The fitting

procedure obtained small ~0.3 % rms errors[76] (the RMS error is not the error for the

moduli) using 28 frequencies to determine two moduli.[77] The estimated errors for the

moduli are 0.09 % for $G$ and 0.33 % for $C_L$ (0.61 % for $B$).

For the RUS fit, the x-ray density was used in the calculation. It is easy to scale to

other densities. Measured thermal expansion (or contraction) was used to correct density

in Fig. 1 for all the phases. The relation in Eq. 1 also can be used for density correction:

$$C(\rho_1) = C(\rho_0)\left(\frac{\rho_1}{\rho_0}\right)^{1/3}, \qquad (1)$$

where $C(\rho_1)$ is the RUS-computed elastic modulus when the sample was assumed to have

the density $\rho_1$.

## III. RESULTS

Table I shows elastic moduli of pure Pu and gallium–stabilized δ-Pu (δ-Pu 2.36 at. % Ga) measured by us at selected temperatures. The elastic moduli of β-Pu and γ-Pu are plotted in Fig. 4. The shear modulus is surprisingly similar between β-Pu and γ-Pu (even more surprising, the shear modulus is slightly larger for γ-Pu) while the bulk modulus decreased at the β–γ transition as expected. γ-Pu resonances were analyzed slightly beyond the temperature range reported previously[21] to its full range of existence (493-616 K).[78] The specimen was measured above 616 K. At 618 K, the dilatometer and resonances exhibited a jump, indicating that it was in the δ-phase. However at the same time, the sample seemed to have lost good contact to the transducers. We were unable to detect a sufficient number of resonances to perform the RUS fit to obtain accurate elastic moduli for δ-Pu. For β-Pu, the temperature dependences of both bulk and shear moduli are quite linear (except at the phase boundaries). Table II contains parameters obtained from linear fits to the measurements of $B$, $G$ and $C_L$. We found that the transition temperatures for α-β, β-γ and γ-δ to be 415 K, 492 K and 617 K, respectively, which are higher than what others found. Thermometry and its errors were described previously.[20]

In Fig. 2, the elastic moduli of α-Pu, β-Pu, and γ-Pu, measured on the same high-quality sample without thermal-cycling are plotted along with the measurements by Linford and Kay[2]. Even accounting for the scatter in the previous study, the larger moduli observed here are expected for higher purity, single-phase material. The bulk moduli (empty diamonds) and shear moduli (solid diamonds) for δ-Pu 2.36 at. % Ga, measured by our group, are also plotted and are consistent with the values of pure Pu because extrapolated values of δ-Pu 2.36 at. % Ga into pure δ-Pu's temperature range are smaller

than that of γ-Pu as expected. We note that the thermal expansion of δ-Pu 2.36 at. % Ga approaches that of pure δ-Pu as gallium content is reduced.[79] δ-Pu 2.36 at. % Ga reported here has a stable δ phase at low temperature.[69]

Table III shows the temperature dependence of the fractional change of the bulk and shear moduli at relatively high temperatures. The temperature dependence of bulk moduli for β-Pu and γ-Pu is unusually small while the temperature dependences of the shear moduli for β-Pu and γ-Pu is similar to both the shear and bulk moduli of α-Pu and δ-Pu 2.36 at. % Ga.

The Varshni function:[80, 81]

$$C(T) = C^0 - \frac{s}{\exp(\theta/T) - 1} \tag{2}$$

is commonly used to fit the temperature dependence of elastic moduli where $C^0$, $s$ and $\theta$ are adjustable parameters. Here, $C^0$ denotes a zero-temperature elastic modulus, $\theta$ is closely related to the Einstein characteristic temperature and $s/2$ is the difference between $C^0$ and the zero-temperature harmonic elastic stiffness coefficient obtained by extrapolating $dC/dT$ linearly from high temperatures.[82, 83] For $T \gg \theta$, the derivative of Eq. 2 is

$$\frac{\partial C(T)}{\partial T} = -\frac{s}{\theta}. \tag{3}$$

The linear extrapolating function from high temperatures is expressed as

$$\tilde{C}(T) = C^0 + \frac{s}{2} - \frac{s}{\theta}T, \tag{4}$$

and $\tilde{C}(\theta/2) = C^0$. Therefore the zero-temperature elastic moduli can be most accurately obtained from high temperature measurements by linear extrapolation to $T=3\Theta_D/8$ where $\theta \approx \Theta_E \approx 3\Theta_D/4$ [84], $\Theta_E$ the Einstein temperature and $\Theta_D$ the Debye temperature.

The Debye temperature, was computed using:[85, 86]

$$\Theta_D = \frac{h}{k} \left( \frac{3}{4\pi V_a} \right)^{1/3} \upsilon_m, \tag{5}$$

where $h$, $V_a$, $k$, and $\upsilon_m$ denote Planck's constant, the atomic volume, Boltzmann's constant, and the mean sound velocity, respectively. We used the X-ray diffraction value[13] for $V_a$ ($\rho = M/N_A V_a$ where $N_A$ is Avogadro's number, and $M=239$ is the atomic weight). The mean sound velocity can be obtained by

$$\upsilon_m = \left[ \frac{1}{3} \left( \frac{1}{\upsilon_l^3} + \frac{2}{\upsilon_t^3} \right) \right]^{-\frac{1}{3}}, \tag{6}$$

where the longitudinal sound velocity, $\upsilon_l = \sqrt{C_L/\rho}$ and the transverse sound velocity, $\upsilon_t = \sqrt{G/\rho}$.

The zero-temperature elastic moduli and $V_a^0$ (estimated value for $V_a$ at 0 K) were used for the computation of $\Theta_D$. $V_a^0$ was estimated by extrapolating the high temperature x-ray and thermal expansion measurements to 0 K using Grüneisen's law:

$$\beta = \frac{\gamma C_P}{V B_S}, \tag{7}$$

where $\beta$ is the isobaric volumetric thermal expansion coefficient, $\gamma$ is the Grüneisen parameter (we hope that context will sort out the double-meaning in this paper of $\beta$ and $\gamma$), $C_P$ is heat capacity at constant pressure, $V$ is volume, and $B_S$ is adiabatic elastic modulus. We assumed $\gamma$ is constant in temperature and $C_P \approx C_V$ where $C_V$ is the heat

capacity at constant volume. We used the Debye model for $C_V$ with Debye temperature computed from Eq. 5. For $B_S$, we used Eq. 2 with our measured bulk modulus.

$B^0$, $G^0$, $V_a^0$ and $\Theta_D$ for β-Pu (and also γ-Pu) were determined numerically using Eqs. 3,4,5,6,7 (Appendix A). We obtained $\Theta_D$=138 K and $V_a^0$=21.2 Å$^3$ for β-Pu ($\Theta_D$=140 K and $V_a^0$=22.3 Å$^3$ for γ-Pu). The zero-temperature elastic moduli are compared to the values derived by Kay, *et al.* using "linear extrapolation to 60 K of data reported by Kay and Linford (1960)[50, 87] (see Table IV). Table V shows comparison to the other phases. We also obtain $\Theta_D^T$ = 109 K for β-Pu using the elastic moduli and $V_a$ at 450 K. We consider $\Theta_D^T$ for comparison because especially α-Pu and δ-Pu 2.36 at. % Ga have strong temperature dependences, i.e. large anharmonic effects.

At higher temperatures, a Grüneisen-Einstein model yields the following expression:[82]

$$\frac{\partial B}{\partial T} = -\frac{3k\gamma(\gamma+1)}{V_a^0}. \tag{8}$$

The Grüneisen parameter, the quintessential measure of anharmonicity, for β-Pu was determined to be $\gamma$= 2.3. The anharmonicities of β-Pu and γ-Pu are more like metals such as copper ($\gamma$= 2.0) while α-Pu and δ-Pu 2.36 at. % Ga have relatively larger values. Wallace estimated $\gamma$ for β-Pu to be much smaller using Eq. 7 (see Table IV).[41] With $\Theta_D^T$=116 K, we calculated the molar $C_V$ of the phonon contribution in the Debye model as 24.9 J·K$^{-1}$·mol$^{-1}$ at 450 K. Using $C_P$-$C_V$=$N_A V_a T\beta^2 B_T$ and $C_P/C_V$= $B_T/B_S$,[88] we have $C_P$ =29.4 J·K$^{-1}$·mol$^{-1}$ from $C_P$=$C_V^2/(C_V-N_A V_a T\beta^2 B_S)$ with $\beta$=1.37×10$^{-4}$ K$^{-1}$·and $V_a$=22.3 Å$^3$, while Oetting *et at.* measured $C_p$=33.3 J·K$^{-1}$·mol$^{-1}$. Their large measured $C_p$ value was attributed to the conduction electrons, anharmonic lattice vibrations, nuclear

characteristics, and magnetic properties.[40] We calculated $\gamma = 2.1$ using our measured $B_S$ and calculated $C_p$ in Eq. 7.

When considering interatomic bonding, Köster and Franz[89] emphasized that Poisson's ratio, $\nu$ is the most relevant elastic parameter. For polycrystalline samples,

$$\nu = \frac{3B - 2G}{2(3B + G)}.$$ 
(9)

In Fig. 5, Poisson's ratios for the three phases of pure Pu as well as δ-Pu 2.36 at. % Ga are plotted as a function of temperature. Poisson's ratio for most materials falls in the range 0.25-0.35.[90] A low Poisson's ratio reflects a high ratio of bond-bending stiffness to bond-stretching stiffness, and a high shear-stiffness to bulk-modulus ratio. Note that Poisson's ratio on warming (Köster and Franz[89]) should increase toward 0.5, characteristic of the liquid state. The Poisson's ratios of aluminum[91, 92], austenitic steel[93], α-Fe[94] and diamond[95, 96] are plotted for comparison.[97] The values and temperature dependence of the Poisson's ratios for β-Pu and γ-Pu are similar to that of many metals while α-Pu has small values and almost no (slightly negative) temperature dependence which is more characteristic of covalent bonding. δ-Pu 2.36 at. % Ga has a value near Fe, but flat temperature dependence. Overall, α-Pu, β-Pu and γ-Pu (and δ-Pu 2.36 at. % Ga) have large differences in their values and temperature dependences as if they are completely different metals.

In Table VI, zero-temperature elastic moduli and the zero-temperature atomic volume for the four phases are compared with theory. Magnetism[98-100] seems to play an important role in theoretical treatments of Pu, but magnetic effects have never been observed. Söderlind *et al.* captures most aspects of the measured behavior while

underestimating the bulk modulus of α-Pu.[38] The ab-initio electronic structure treatments of Pu are, at their core, zero-temperature ones. The unusually low elastic moduli observed here require that entropic considerations are essential in understanding the phases of Pu, especially in light of the very low elastic moduli. Such effects are absent in most ab-initio models. In Table VII, theoretical predictions for bulk modulus are compared with our data for the four phases. The calculated values by the atomistic model[39] are in good agreement with our data.

## IV. CONCLUSIONS

We have reported accurate elastic moduli of pure polycrystalline β plutonium of its entire existence temperature range at ambient pressure. The elastic response of pure β-Pu, when compared to other phases of Pu and to other metals, displays many bizarre features including an increase (albeit small) in shear modulus on warming from β to γ, and Poisson's ratios that differ strongly among the three phases explored here. These measured properties support the conjecture that Pu lies on a knife-edge of stability caused by the 5f electrons.

# REFERENCES

1.  S. S. Hecker, Metall Mater Trans A **35A**, 2207 (2004).

2.  O. J. Wick, *Plutonium Handbook*. (Gordon and Breach, New York, 1967).

3.  A. Goldberg and T. B. Massalski, in *Plutonium 1970 and Other Actinides*, edited by W. N. Miner (The Metallurgical Society of the American Institute of Mining, New York, 1970), Vol. 2, p. 875.

4.  J. J. Rechtien and R. D. Nelson, Met. Trans. **4**, 2755 (1973).

5.  T. A. Sandenaw, Journal of Nuclear Materials **73**, 204 (1978).

6.  J. C. Lashley, M. S. Blau, K. P. Staudhammer and R. A. Pereyra, Journal of Nuclear Materials **274**, 315 (1999).

7.  P. Soderlind, O. Eriksson, B. Johansson, J. M. Wills and A. M. Boring, Nature **374**, 524 (1995).

8.  R. C. Albers, Nature **410**, 759 (2001).

9.  G. H. Lander, Science **301**, 1057 (2003).

10. R. C. Albers and J.-X. Zhu, Nature **446**, 504 (2007).

11. K. T. Moore and G. van der Laan, Reviews of Modern Physics **81**, 235 (2009).

12. W. H. Zachariasen and F. H. Ellinger, Acta Cryst. **16**, 777 (1963).

13. W. H. Zachariasen and F. H. Ellinger, Acta Cryst. **12**, 175 (1959).

14. W. H. Zachariasen and F. H. Ellinger, Acta Cryst. **8**, 431 (1955).

15. F. H. Ellinger, Journal of Metals **80**, 1256 (1956).

16. R. O. Elliott and A. C. Larson, in *The Metal Plutonium*, edited by A. S. Coffinberry and W. N. Miner (ASM, Metals Park, 1961), p. 265.

17. J. C. Z. Serpan and L. J. Wittenberg, Metallurgical Society of American Institute of Mining, Metallurgical and Petroleum Engineers -- Transactions **221**, 1017 (1961).

18. W. N. Miner and F. W. Schonfeld, in *Plutonium Handbook*, edited by O. J. Wick (Gorden and Breach, New York, 1967), p. 31.

19. H. Ledbetter, A. Migliori, J. Betts, S. Harrington and S. El-Khatib, Phys Rev B **71**, 172101 (2005).

20. A. Migliori, C. Pantea, H. Ledbetter, I. Stroe, J. B. Betts, J. N. Mitchell, M. Ramos, F. Freibert, D. Dooley, S. Harrington and C. H. Mielke, J Acoust Soc Am **122**, 1994 (2007).

21. I. Stroe, J. B. Betts, A. Trugman, C. H. Mielke, J. N. Mitchell, M. Ramos, F. J. Freibert, H. Ledbetter and A. Migliori, J Acoust Soc Am **127**, 741 (2010).

22. A. Migliori, H. Ledbetter, A. C. Lawson, A. P. Ramirez, D. A. Miller, J. B. Betts, M. Ramos and J. C. Lashley, Phys Rev B **73**, 052101 (2006).

23. A. Migliori, I. Mihut-Stroe and J. B. Betts, Materials Research Society Symposium Proceedings - Actinides 2008 - Basic Science, Applications and Technology **1104**, 249 (2008).

24. H. L. Skriver, O. K. Andersen and B. Johansson, Phys Rev Lett **41**, 42 (1978).

25. P. Soderlind, Europhys Lett **55**, 525 (2001).

26. S. Y. Savrasov, G. Kotliar and E. Abrahams, Nature **410**, 793 (2001).

27. X. Dai, S. Y. Savrasov, G. Kotliar, A. Migliori, H. Ledbetter and E. Abrahams, Science **300**, 953 (2003).

28. P. Söderlind and B. Sadigh, Phys Rev Lett **92**, 185702 (2004).

29. G. van der Laan, K. T. Moore, J. G. Tobin, B. W. Chung, M. A. Wall and A. J. Schwartz, Phys Rev Lett **93**, 097401 (2004).

30. L. V. Pourovskii, M. I. Katsnelson, A. I. Lichtenstein, L. Havela, T. Gouder, F. Wastin, A. B. Shick, V. Drchal and G. H. Lander, Europhys Lett **74**, 479 (2006).

31. K. T. Moore, P. Soderlind, A. J. Schwartz and D. E. Laughlin, Phys Rev Lett **96**, 206402 (2006).

32. J. H. Shim, K. Haule and G. Kotliar, Nature **446**, 513 (2007).

33. P. Söderlind, Phys Rev B **77**, 085101 (2008).

34. C. D. Batista, J. E. Gubernatis, T. Durakiewicz and J. J. Joyce, Phys Rev Lett **101**, 016403 (2008).

35. T. Lookman, A. Saxena and R. C. Albers, Phys Rev Lett **100**, 145504 (2008).

36. P. Söderlind and J. E. Klepeis, Phys Rev B **79**, 104110 (2009).

37. Y. K. Vekilov and O. M. Krasilnikov, Journal of Experimental and Theoretical Physics **109**, 446 (2009).

38. P. Söderlind, A. Landa, J. E. Klepeis, Y. Suzuki and A. Migliori, Phys Rev B **81**, 224110 (9 pp.) (2010).

39. M. I. Baskes, Phys Rev B **62**, 15532 (2000).

40. F. L. Oetting and R. O. Adams, The Journal of Chemical Thermodynamics **15**, 537 (1983).

41. D. C. Wallace, Phys Rev B **58**, 15433 (1998).

42. J. C. Lashley, J. Singleton, A. Migliori, J. B. Betts, R. A. Fisher, J. L. Smith and R. J. McQueeney, Phys Rev Lett **91**, 205901 (2003).

43. R. J. McQueeney, A. C. Lawson, A. Migliori, T. M. Kelley, B. Fultz, M. Ramos, B. Martinez, J. C. Lashley and S. C. Vogel, Phys Rev Lett **92**, 146401 (2004).

44. T. G. Zocco, D. S. Schwartz and J. Park, Journal of Nuclear Materials **353**, 119 (2006).

45. C. A. Alexander and V. E. Wood, J Appl Phys **103**, 063704 (2008).

46. M. Boivineau, Journal of Nuclear Materials **392**, 568 (2009).

47. A. Filanovich, A. Povzner, V. Bodryakov, Y. Tsiovkin and V. Dremov, Technical Physics Letters **35**, 929 (2009).

48. F. J. Freibert, J. N. Mitchell, T. A. Saleh and D. S. Schwartz, IOP Conference Series: Materials Science and Engineering **9**, 012096 (2010).

49. B. Fultz, Progress in Materials Science **55**, 247 (2010).

50. A. E. Kay and P. F. T. Linford, in *Plutonium 1960* (Cleaver-Hume, London, 1961).

51. F. W. Schonfeld, in *Plutonium 1960*, edited by E. Grison, W. B. Lord and R. D. Fowler (Cleaver-Hume, London, 1961).

52. H. R. Gardner, in *Plutonium Handbook*, edited by O. J. Wick (The American Nuclear Society, La Grange Park, 1980), Vol. 1.

53. H. R. Gardner and I. B. Mann, in *Plutonium 1960*, edited by E. Grison, W. B. Lord and R. D. Fowler (Cleaver-Hume, London, 1961).

54. J. A. Cornet and J. M. Bouchet, Journal of Nuclear Materials **28**, 303 (1968).

55. P. W. Bridgman, J Appl Phys **30**, 214 (1959).

56. A. S. Coffinberry and M. B. Waldron, Progr. of Nuclear Energy V **1**, 354 (1956).

57. A. S. Coffinberry and M. B. Waldron, in *Metallurgy and fuels*, edited by H. M. Finniston and J. P. Howe (Pergamon Press, London, 1956).

58. J. F. Andrew and J. R. Morgan, Journal of Nuclear Materials **19**, 115 (1966).

59. R. Lallement, Phys Lett **5**, 182 (1963).

60. R. Lallement and P. Solente, in *Plutonium 1965*, edited by A. E. Kay and M. B. Waldron (Institute of Metals, London, 1965), p. 147.

61. J. Taylor, R. G. Loasby, D. J. Dean and P. F. Linford, in *Plutonium 1965*, edited by A. E. Kay and M. B. Waldron (Institute of Metals, London, 1967), p. 162.

62. M. Rosen, G. Erez and S. Shtrikman, Phys Rev Lett **21**, 430 (1968).

63. C. A. Calder, E. C. Draney and W. W. Wilcox, J. Nucl. Mater. **97**, 126 (1981).

64. M. Rosen, L. T. Lloyd and R. G. Petersen, in *Plutonium 1965*, edited by A. E. Kay and M. B. Waldron (Institute of Metals, London, 1967), p. 18.

65. J. E. Selle and A. E. Focke, Journal of Nuclear Materials **33**, 149 (1969).

66. H. M. Ledbetter and R. L. Moment, Acta Metallurgica **24**, 891 (1976).

67. J. Wong, M. Krisch, D. L. Farber, F. Occelli, A. J. Schwartz, T.-C. Chiang, M. Wall, C. Boro and R. Xu, Science **301**, 1078 (2003).

68. R. B. Roof, Advances in X-Ray Analysis **24**, 221 (1981).

69. A. Migliori, F. Freibert, J. C. Lashley, A. C. Lawson, J. P. Baiardo and D. A. Miller, J Supercond **15**, 499 (2002).

70. A. Migliori, I. Mihut, J. B. Betts, M. Ramos, C. Mielke, C. Pantea and D. Miller, J Alloy Compd **444-445**, 133 (2007).

71. A. Migliori, J. L. Sarrao, W. M. Visscher, T. M. Bell, M. Lei, Z. Fisk and R. G. Leisure, Physica B **183**, 1 (1993).

72. A. Migliori and J. Sarrao, *Resonant Ultrasound Spectroscopy*. (Wiley-Interscience, New York, 1997).

73. A. Migliori and J. D. Maynard, Rev Sci Instrum **76**, 121301 (2005).

74. One data point was measured between the alpha and beta phases at 415 K. The resonance frequencies at this temperature were not resembling either ones of the alpha nor beta phase. The RUS fit produced the elastic moduli between the two phases. The density correction was done using the average density of the alpha

and beta phases. Please note that this uncertainty in density gives only ± 2 % errors in elastic moduli, and Poisson's ratio is not affected by density change.

75. The two lowest resonances were below this frequency range. They were recorded for a few temperatures for which we used a larger frequency range. For them, the value difference in the elastic moduli which were derived with the two lowest resonances (30 resonances total) or without them (28 resonances total) were negligible. Therefore, the elastic moduli for all temperatures were obtained without the lowest two resonances.

76. The codes used for the calculation available at [http://www.magnet.fsu.edu/inhouseresearch/rus/index.html (date last viewed 01/28/11)].

77. The RUS fit program in ref 76 also have capacity to fit the sample dimensions. For a consistency check, four parameters (two elastic moduli and two relative dimensions) were fit. The result showed the negligible change in elastic moduli and dimensions, and the rms errors were slightly smaller.

78. The measured resonant frequency values were used directly for the RUS fit unlike ref. 21, in which, the resonant frequencies were linearly fitted as a function of temperature before the RUS fit.

79. A. C. Lawson, J. A. Roberts, B. Martinez and J. W. J. Richardson, Philosophical Magazine B **82**, 1837 (2002).

80. G. Leibfried and L. Ludwig, *Solid State Physics*. (Academic, New York, 1961).

81. Y. P. Varshni, Phys Rev B **2**, 3952 (1970).

82. H. Ledbetter, physica status solidi (b) **181**, 81 (1994).

83. H. Ledbetter, Materials Science and Engineering A **442**, 31 (2006).

84. L. A. Girifalco, *Statistical Mechanics of Solids*. (Oxford University Press, New York, 2000).

85. M. Blackman, *Handbuch der Physik*. (Springer, Berlin, 1955).

86. H. Ledbetter, Zeitschrift fuer Metallkunde/Materials Research and Advanced Techniques **82**, 820 (1991).

87. A. E. Kay and R. G. Loasby, Philos Mag **9**, 37 (1964).

88. D. C. Wallace, *Thermodynamics of Crystals*. (Dover, Mineola, 1972).

89.     W. Koester and H. Franz, Metallurgical Reviews **6**, 1 (1961).

90.     K. Gschneidner, *Solid State Physics*. (Academic, New York, 1964).

91.     G. N. Kamm and G. A. Alers, J Appl Phys **35**, 327 (1964).

92.     J. L. Tallon and A. Wolfenden, J Phys Chem Solids **40**, 831 (1979).

93.     A. Moreau, S. E. Kruger, M. Cote and P. Bocher, 1st International Symposium on Laser Ultrasonics: Science, Technology and Applications (2008).

94.     S. A. Kim and W. L. Johnson, Mat Sci Eng a-Struct **452**, 633 (2007).

95.     A. Migliori, H. Ledbetter, R. G. Leisure, C. Pantea and J. B. Betts, J Appl Phys **104**, 053512 (2008).

96.     E. S. Zouboulis, M. Grimsditch, A. K. Ramdas and S. Rodriguez, Phys Rev B **57**, 2889 (1998).

97.     Poisson's ratios for polycrystalline samples were calculated using the single crystal elastic moduli in the references.

98.     J. C. Lashley, A. Lawson, R. J. McQueeney and G. H. Lander, Phys Rev B **72**, 054416 (2005).

99.     A. Z. Solontsov, V. K. Orlov, S. A. Kiselev and A. A. Burmistrov, Atomic Energy **107**, 263 (2009).

100.    R. H. Heffner, G. D. Morris, M. J. Fluss, B. Chung, S. McCall, D. E. MacLaughlin, L. Shu, K. Ohishi, E. D. Bauer, J. L. Sarrao, W. Higemoto and T. U. Ito, Phys Rev B **73**, 094453 (2006).

101.    F. W. Schonfeld and R. E. Tate, Report LA-13034-MS (1996).

102.    H. Ledbetter, A. Lawson and A. Migliori, Journal of Physics: Condensed Matter **22**, 165401 (2010).

103.    G. Robert, A. Pasturel and B. Siberchicot, J Phys-Condens Mat **15**, 8377 (2003).

104.    A. L. Kutepov and S. G. Kutepova, J Magn Magn Mater **272-276**, e329 (2004).

105.    E. M. Cramer, L. L. Hawes, W. N. Miner and F. W. Schonfeld, in *The Metal Plutonium*, edited by A. S. Coffinberry and W. N. Miner (ASM, Metals Park, 1961), p. 112.

106.    J. A. Lee and P. G. Mardon, in *The Metal Plutonium*, edited by A. S. Coffinberry and W. N. Miner (ASM, Metals Park, 1961), p. 133.

107.   T. A. Sandenaw, in *Plutonium 1960*, edited by E. Grison, W. B. Lord and R. D. Fowler (Cleaver-Hume, London, 1961), p. 79.

108.   A. C. Lawson, J. A. Goldstone, B. Cort, R. I. Sheldon and E. M. Foltyn, J. Alloys & Componds **213-14**, 426 (1994).

109.   A. B. Shick and et al., EPL (Europhysics Letters) **69**, 588 (2005).

110.   A. C. Lawson, B. Cort, J. A. Roberts, B. I. Bennett, T. O. Brun, R. B. Von Dreele and J. W. J. Richardson, in *1998 Winter Meeting of American Nuclear Society*, edited by A. Gonis, N. Kioussis and M. Ciftan (Kluwe-Plenum, New York, 1999), p. 75.

111.   Y. Wang and Y. F. Sun, J Phys-Condens Mat **12**, L311 (2000).

112.   F. Freibert, D. Dooley and D. Miller, Report No.: LAUR-05-9007 (2005).

**Appendix A**

Using measured high temperature elastic moduli, we estimated the zero-temperature elastic moduli, the zero-temperature atomic volume and the Debye temperature with the most accurate method we are aware of. From the high temperature measurements where the elastic moduli are linear in temperature (Eq. 2), using three measured values: $T_1$, $C_1$ and $C'_1$ (where $C_1 = C(T_1)$ is elastic modulus and $C'_1 = dC(T)/dT\,|_{T=T_1}$ ), from Eq. 4, the zero-temperature elastic modulus can be estimated:

$$C^0 = C_1 + C'_1(\frac{3}{8}\Theta_D - T_1). \tag{10}$$

From Eq. 5 and 6,

$$\Theta_D = \left(\frac{9}{4\pi}\right)^{1/3} \frac{h}{k} \sqrt{\frac{N_A}{M}} V_a^{1/6} \left(\left[C_{L1} + C'_{L1}(\frac{3}{8}\Theta_D - T_1)\right]^{-3/2} + 2\left[G_1 + G'_1(\frac{3}{8}\Theta_D - T_1)\right]^{-3/2}\right)^{-\frac{1}{3}}. \tag{11}$$

Table VIII lists the values of $C_{L1}$, $C_{L'1}$, $G_1$, $G'_1$ , and $T_1$ for β-Pu and γ-Pu that we used. The right-hand side of Eq. 11 was calculated numerically starting with $\Theta_D$=100 K and iterated.

Eq. 11 is a very slowly varying function of $V_a$. A 5 % error in $V_a$ yields less than 1 % error in $\Theta_D$. The temperature dependence of $V_a$ for β-Pu and γ-Pu in Fig 1 suggests that $V_a$ at 0 K should be within 5 % of that at higher temperature, so that $V_a$ at high temperature can be used safely to estimate $\Theta_D$. This estimation of the zero-temperature $V_a$ is most useful for comparison with first-principles calculations.

To estimate $V_a^0$, we took, again, three values from the thermal expansion measurement: $T_1$, $V_1$ and $V'_1$ (where $V_1=V(T_1)$ is the volume and $V'_1 = dV(T)/dT\,|_{T=T_1}$ ).

Similar to what we did for elastic moduli, we need to find ratio of temperature to Debye temperature, $\varepsilon$, and then extrapolate to find $V^0$,

$$V^0 = V_1 + V_1'(\varepsilon\,\Theta_D - T_1).\tag{12}$$

From Eq. 7:

$$\beta(T) = \frac{1}{V(T)}\frac{dV(T)}{dT} = \frac{\gamma C_P(T)}{V(T)B_S(T)}.\tag{13}$$

We approximated $C_P \approx C_V$ (or $B_T \approx B_S$) because we measured $B_S$, but with measurements of $B_T$, the approximation is not necessary because $\beta = \gamma C_P/VB_S = \gamma C_V/VB_T$. The volume at $T_1$ can be calculated as:

$$V(T_1) = \int_0^{T_1} \frac{\gamma C_V(T)}{B(T)}dT + V(0),\tag{14}$$

If we assume that the temperature dependence of $B(T)$ is negligible, and use the Debye model for $C_V(T)$, we have $\varepsilon = 0.375$ for $T_1 \gg \Theta_D$. However, the contribution from softening of $B(T)$ to $V(T)$ is rather large and increases the values of $\varepsilon$ away from 0.375 at high temperature.

From Eq. 2 to 4,

$$B(T) = B^0\left(1 - \frac{\delta}{\exp(3\Theta_D/4T)-1}\right),\tag{15}$$

where

$$\delta = \frac{s}{B^0} = -\frac{3\Theta_D B_1'}{4B^0} = -\frac{3\Theta_D B_1'}{4\left[B_1 + B_1'\left(\dfrac{3\Theta_D}{8} - T_1\right)\right]}.\tag{16}$$

$\delta$ is ~0.05-0.1 for typical metals as well as for β-Pu (0.039) and γ-Pu (0.037). $V'(T)$ also never converges at $T \gg \Theta_D$. Therefore, $\varepsilon$ is a function of $\delta$ and $n$ where $n = T_1/\Theta_D$. It can be

solved numerically for $\varepsilon$ for known values of $\delta$ and $n$. The solutions of $\varepsilon$ for different

$\delta$ and $n$ are displayed in Table IX. For convenience, the values for $\varepsilon$ can be approximated

within a few % error for $n > 1.5$ by the function:

$$\varepsilon \approx 0.311 + 0.0128n - 5.68 \times 10^{-3} n^2 + 5.28 \times 10^{-4} n^3 - \left(2.01 + 0.119n - 1.18n^2 + 0.0530n^3\right)\delta$$
$$- \left(35.4 - 63.6n + 24.9n^2 - 1.85n^3\right)\delta^2 + \left(131 - 163n + 25.5n^2 + 7.82n^3\right)\delta^3 \qquad . (17)$$

The zero-temperature atomic volume is

$$V_a^0 = V_a^T \frac{V^0}{V_1} = V_a^T \left(1 + \frac{V_1'(\varepsilon\,\Theta_D - T_1)}{V_1}\right) = V_a^T \left(1 + \beta(T_1)[\varepsilon\,\Theta_D - T_1]\right), \qquad (18)$$

where $V_a^T$ is the atomic volume at $T_1$ obtained from the measurement (see table V) and

$\beta(T_1) = V'_1/V_1$. $V_a$ in Eq. 11 can be replace by $V_a^0$ in Eq. 18 and more accurate values for

$C_L^0$, $G^0$, $V_a^0$ and $\Theta_D$ can be obtained by iterating Eq. 11.

This method was tested on α-Pu. Our elastic modulus measurement and the

thermal expansion measurement[101] for 380±10 K were used (see table VIII) to extract the

zero-temperature parameters. $\delta$=0.150 for α-Pu and it is much larger than for β-Pu and γ-

Pu. Table X contains the comparison to measured values. At $T_1$=380 K, $n$=1.85 and it is

at the lower limit for Eq. 3 to work. Still, this method produced excellent predictions for

zero-temperature parameters using the measured values at 380 K in the 20 K window.

**TABLES**

**TABLE I.** Elastic moduli ($B$: bulk, $G$: shear, $C_L$: longitudinal and $E$: Young's modulus) and $\nu$ (Poisson's ratio) of pure $\alpha$-Pu[19, 20], $\beta$-Pu[38] and $\gamma$-Pu[21] and $\delta$-Pu 2.36 at. % Ga[23] at selected temperatures.

| Temperature (K) | Phase | $B$ (GPa) | $G$ (GPa) | $C_L$ (GPa) | $E$ (GPa) | $\nu$ |
|---|---|---|---|---|---|---|
| 18.36 |  | 72.28 | 58.91 | 150.82 | 138.97 | 0.1795 |
| 95.82 |  | 69.03 | 56.36 | 144.18 | 132.90 | 0.1791 |
| 203.3 | $\alpha$ | 62.56 | 51.24 | 130.88 | 120.75 | 0.1783 |
| 297.9 |  | 55.93 | 45.85 | 117.05 | 108.02 | 0.1781 |
| 407.0 |  | 48.17 | 39.91 | 101.39 | 93.82 | 0.1754 |
| 415.0 | $\alpha$–$\beta$[*] | 35.81 | 23.74 | 67.46 | 58.33 | 0.2285 |
| 417.0 |  | 34.36 | 18.22 | 58.65 | 46.44 | 0.2748 |
| 451.0 | $\beta$ | 33.80 | 17.09 | 56.59 | 43.89 | 0.2836 |
| 491.0 |  | 33.11 | 16.12 | 54.60 | 41.61 | 0.2905 |
| 493.0 |  | 25.72 | 16.51 | 47.74 | 40.81 | 0.2356 |
| 551.0 | $\gamma$ | 24.96 | 15.19 | 45.22 | 37.89 | 0.2470 |
| 616.0 |  | 24.23 | 14.00 | 42.90 | 35.21 | 0.2578 |
|  |  |  |  |  |  |  |
| 14.63 |  | 37.77 | 20.18 | 64.68 | 51.39 | 0.2732 |
| 94.48 |  | 36.21 | 19.43 | 62.12 | 49.45 | 0.2724 |
| 203.8 |  | 33.46 | 18.00 | 57.46 | 45.79 | 0.2719 |
| 299.9 | $\delta$[**] | 30.80 | 16.39 | 52.65 | 41.76 | 0.2740 |
| 400.9 |  | 27.13 | 14.43 | 46.37 | 36.77 | 0.2741 |
| 451.2 |  | 25.48 | 13.49 | 43.47 | 34.40 | 0.2750 |
| 496.0 |  | 24.11 | 12.78 | 41.15 | 32.58 | 0.2748 |

[*] See ref 74.  [**] $\delta$-Pu 2.36 at. % Ga.

**TABLE II**. Parameters obtained for linear fits to the measurements of $B$, $G$ and $C_L$ of the form $a + bT$ for β-Pu from 421 to 487 K.

| Elastic Modulus | $a$ (GPa) | $b$ (GPa/K) |
|---|---|---|
| $B$ | 40.58 | -0.01509 |
| $G$ | 26.07 | -0.01990 |
| $C_L$ | 75.34 | -0.04162 |

s

**TABLE III**. Comparison of the fractional changes of the bulk and shear moduli with temperature at relatively high temperatures. The temperature dependence of bulk moduli for β-Pu and γ-Pu is unusually small. The others values are quite similar to each other.

| Phase | α (380 K)[*] | β (450 K) | γ (550 K)[*] | δ (480 K)[*] |
|---|---|---|---|---|
| $-dB/BdT$ (K$^{-1}$) | $1.4 \times 10^{-3}$ | $0.4 \times 10^{-3}$ | $0.4 \times 10^{-3}$ | $1.3 \times 10^{-3}$ |
| $-dG/GdT$ (K$^{-1}$) | $1.4 \times 10^{-3}$ | $1.2 \times 10^{-3}$ | $1.4 \times 10^{-3}$ | $1.2 \times 10^{-3}$ |

[*] Ref 18.

**TABLE IV**. The zero-temperature elastic moduli, the Debye temperatures, and the Grüneisen parameters, for β-Pu compared to literature values.

| Parameter / Method | $B^0$ (GPa) | $G^0$ (GPa) | $C_L^0$ (GPa) | $\Theta_D$ (K) | $\gamma$ |
|---|---|---|---|---|---|
| Kay (elastic moluli)[87] | 46.2 | 24 | 78 | 133 | - |
| Wallace ($\gamma = V\beta B_S/C_P$)[41] | - | - | - | - | 1.4 |
| our calculation ($\gamma = V\beta B_S/C_P$) | - | - | - | - | 2.1 |
| present (elastic moduli) | 39.8 | 25.0 | 73.2 | 138 | 2.3 |

24

**TABLE V**. The Debye temperatures, (computed from the zero-temperature elastic moduli* and $V_a^0$), $\Theta_D^T$ (computed from the measured elastic moduli and $V_a^T$ at high temperatures), and the Grüneisen parameters are compared for the different phases[19-21, 23, 102].

| Parameter / Phase | $V_a^0$ (Å$^3$) | $\Theta_D$ (K) | $V_a^T$ (Å$^3$) | $\Theta_D^T$ (K) | $\gamma$ |
|---|---|---|---|---|---|
| α | 19.4 | 207 | 20.3 (380 K) | 175 (380 K) | 5.2 (380 K) |
| β | 21.2** | 138 | 22.3 (450 K) | 116 (450 K) | 2.3 (450 K) |
| γ | 22.3** | 140 | 23.3 (550 K) | 109 (550 K) | 1.9 (550 K) |
| δ*** | 24.5 | 115 | 24.7 (650 K) | 91 (650 K) | 3.8 (480 K) |

* The values are shown in Table VI.

** Estimated value for $V_a$ at 0K.

*** δ-Pu 2.36 at. % Ga was used. $\Theta_D^T$ was derived by extrapolating the elastic modulus values to 650 K at which the δ phase of pure Pu exists. The values for δ-Pu 2 at. % Ga in ref. 79 were used for $V_a^0$ and $V_a$ at 650 K.

**TABLE VI**. The zero-temperature elastic moduli and the zero-temperature atomic volume for four phases of Pu are compared with other results.

| Phase | | Method / Parameter | $B^0$ (GPa) | $G^0$ (GPa) | $C_L^0$ (GPa) | $V_a^0$ (Å$^3$) |
|---|---|---|---|---|---|---|
| α | theory | Robert (Non-spin-polarized)[103] | 169.2 | - | - | 18.10 |
| | | Robert (Spin-polarized AFM)[103] | 101.1 | - | - | 18.47 |
| | | Kutepov (NM)[104] | 175.4 | - | - | 18 |
| | | Kutepov (AFM)[104] | 119 | - | - | 18 |
| | | Söderlind (SO)[38] | 30.6 | 49.9 | 97.1 | 19.0 |
| | | Söderlind (SO+OP)[38] | 34.4 | 51.3 | 102.8 | 20.3 |
| | experiment | Kay (ultrasonic resonance)[87] | 70 | 50 | 136 | - |
| | | our result (RUS)[20] | 72.0 | 58.6 | 150.2 | - |
| | | (x-ray[12], dilatometry[105-108]) | - | - | - | 19.4 |

| | | | | | | |
|---|---|---|---|---|---|---|
| β | theory | Söderlind (SO)[38] | 36.0 | 26.2 | 70.9 | 22.0 |
| | | Söderlind (SO+OP)[38] | 38.5 | 25.3 | 72.2 | 23.1 |
| | experiment | Kay (ultrasonic resonance)[87] | 46.2 | 24 | 78 | - |
| | | our result (RUS) | 39.8 | 25.0 | 73.2 | - |
| | | our calculation[*] | - | - | - | 21.2 |
| γ | theory | Robert (Non-spin-polarized)[103] | 129.2 | - | - | 18.20 |
| | | Robert (Spin-polarized AFM I)[103] | 35.2 | - | - | 22.14 |
| | | Robert (Spin-polarized AFM II)[103] | 44.4 | - | - | 21.90 |
| | | Söderlind (SO)[38] | 36.5 | 26.4 | 71.7 | 22.7 |
| | | Söderlind (SO+OP)[38] | 34.6 | 22.2 | 64.2 | 23.8 |
| | experiment | Kay (ultrasonic resonance)[87] | 40.6 | 24 | 73 | - |
| | | our result (RUS) | 30.3 | 25.6 | 64.4 | - |
| | | our calculation[*] | - | - | - | 22.3 |
| δ | theory | Robert (Non-spin-polarized)[103] | 99.9 | - | - | 19.57 |
| | | Robert (Spin-polarized AFM)[103] | 54.8 | - | - | 23.43 |
| | | Kutepov (NM)[104] | 90.7 | - | - | 20 |
| | | Kutepov (AFM)[104] | 51.0 | - | - | 24 |
| | | Shick (LSDA)[109] | 76.1 | - | - | 20 |
| | | Shick (FLL LSDA+U)[109] | 67.5 | - | - | 28 |
| | | Shick (AMF LSDA+U)[109] | 31.4 | - | - | 27 |
| | | Söderlind (SO)[38] | 39.0 | 27.8 | 76.0 | 24.2 |
| | | Söderlind (SO+OP)[38] | 41.0 | 30.6 | 81.8 | 24.9 |
| | | Söderlind (EMTO)[38] | 39.6 | 42.3 | 96.0 | 25.5 |
| | experiment | Kay (ultrasonic resonance)[87] | 51 | 19 | 77 | - |
| | | our result (RUS)[**, 23] | 37.8 | 20.2 | 64.7 | - |
| | | Lawson[***, 79] | - | - | - | 24.8 |

[*] (x-ray[13, 14], dilatometry, RUS[20, 21]).   [**] δ-Pu 2.36 at. % Ga was used.

[***] (neutron diffraction[110]) calculated value for non-alloyed δ-Pu based on the Invar model.

**TABLE VII**. Calculated bulk moduli with thermodynamic effects are compared with our measurments[19, 21, 23].

| Method \ Phase | α (294 K) | β (388 K) | γ (508 K) | δ (593 K) | δ (650 K) |
|---|---|---|---|---|---|
| Baskes (EAM)[39] | 41 | 31 | 23 | 25 | - |
| Wang (CMF)[111] | - | - | - | - | 43.0 |
| our result (RUS) | 56.2 | 34.7[*] | 25.6 | 21.5[*, **] | 19.9[*, **] |

[*] The extrapolated values.  [**] δ-Pu 2.36 at. % Ga was used.

**TABLE VIII**. $T_1$, $C_{L1}$, $C_{L1}$', $G_1$, $G_1$' $B_1$, $B_1$' and $\beta$ for β-Pu and γ-Pu (and α-Pu for testing) which we used for Eq. 11, 12 and 16. $C_{L1}$, $C_{L1}$', $G_1$, $G_1$' $B_1$ and $B_1$' were extracted from our measurements for $T_1 \pm 20$ ($\pm 10$ for α-Pu) K.  $\beta(T_1)$ were extracted from ref. 101 which summarizes the best previous thermal expansion and x-ray measurements of pure Pu.

| Data \ Phase | $T_1$ (K) | $C_{L1}$ (GPa) | $C_L{'}_1$ (GPa/K) | $G_1$ (GPa) | $G'_1$ (GPa/K) | $B_1$ (GPa) | $B'_1$ (GPa/K) | $\beta \times 10^{-4}$ (K$^{-1}$) |
|---|---|---|---|---|---|---|---|---|
| β-Pu | 450 | 56.6 | -0.0416 | 17.1 | -0.0199 | 33.8 | -0.0151 | 1.37 |
| γ-Pu | 550 | 45.2 | -0.0386 | 15.2 | -0.0210 | 25.0 | -0.0106 | 1.04 |
| α-Pu | 380 | 105.3 | -0.1416 | 41.4 | -0.0545 | 50.1 | -0.0689 | 1.92 |

**TABLE IX**. The solutions for $\varepsilon$ for different $\delta$ and $n$ values using Eq. 12 to 15.

| $n$ / $\delta$ | 1 | 2 | 3 | 4 | 5 | 6 | 7 | 8 | 9 | 10 |
|---|---|---|---|---|---|---|---|---|---|---|
| 0.01 | 0.295 | 0.348 | 0.391 | 0.441 | 0.502 | 0.576 | 0.664 | 0.765 | 0.881 | 1.012 |
| 0.02 | 0.298 | 0.367 | 0.440 | 0.534 | 0.655 | 0.806 | 0.986 | 1.20 | 1.44 | 1.72 |
| 0.05 | 0.308 | 0.425 | 0.593 | 0.835 | 1.16 | 1.58 | 2.11 | 2.76 | 3.54 | 4.48 |
| 0.075 | 0.316 | 0.476 | 0.731 | 1.11 | 1.65 | 2.38 | 3.33 | 4.59 | 6.28 | 8.78 |
| 0.10 | 0.324 | 0.529 | 0.879 | 1.43 | 2.24 | 3.40 | 5.13 | - | - | - |
| 0.15 | 0.342 | 0.642 | 1.22 | 2.22 | 4.04 | - | - | - | - | - |
| 0.20 | 0.360 | 0.767 | 1.64 | 3.60 | - | - | - | - | - | - |

**TABLE X**. The test for our method of calculation for extracting zero-temperature parameters using measured data[*] at 380±10 K for α-Pu. The extracted values are compared to the measured values[19] at low temperature.

| Parameter / Method | $B^0$ (GPa) | $G^0$ (GPa) | $C_L^0$ (GPa) | $\Theta_D$ (K) | $V_a^0$ (Å³) |
|---|---|---|---|---|---|
| measurement | 72.0 | 58.6 | 150.2 | 207 | 19.4 |
| our calculation | 71.0 | 57.9 | 148.2 | 205 | 19.4 |

[*] The values are shown in Table VIII.
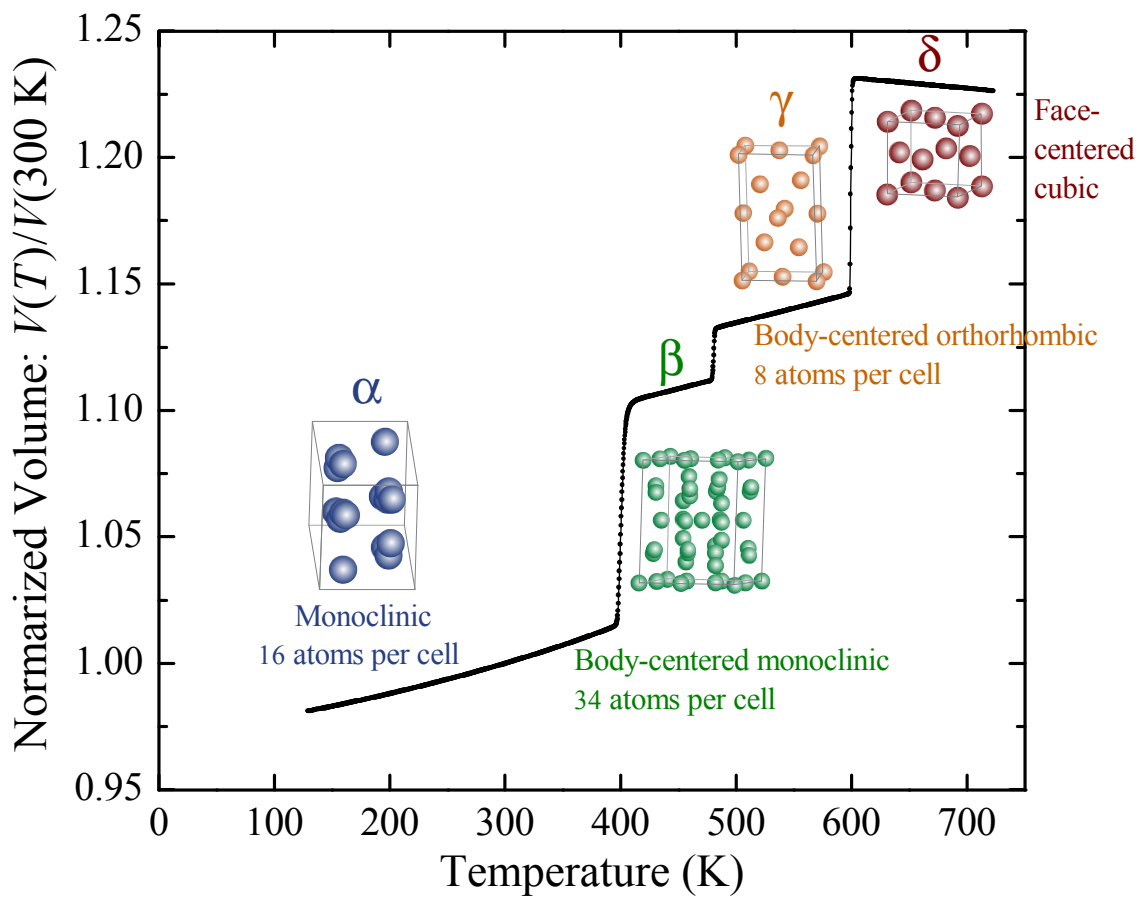
**Figure 1.** Normalized volume of pure Pu relative to 300 K was derived from dilatometer measurements and is plotted from 120 to 720 K for α-Pu, β-Pu, γ-Pu and δ-Pu.[112]
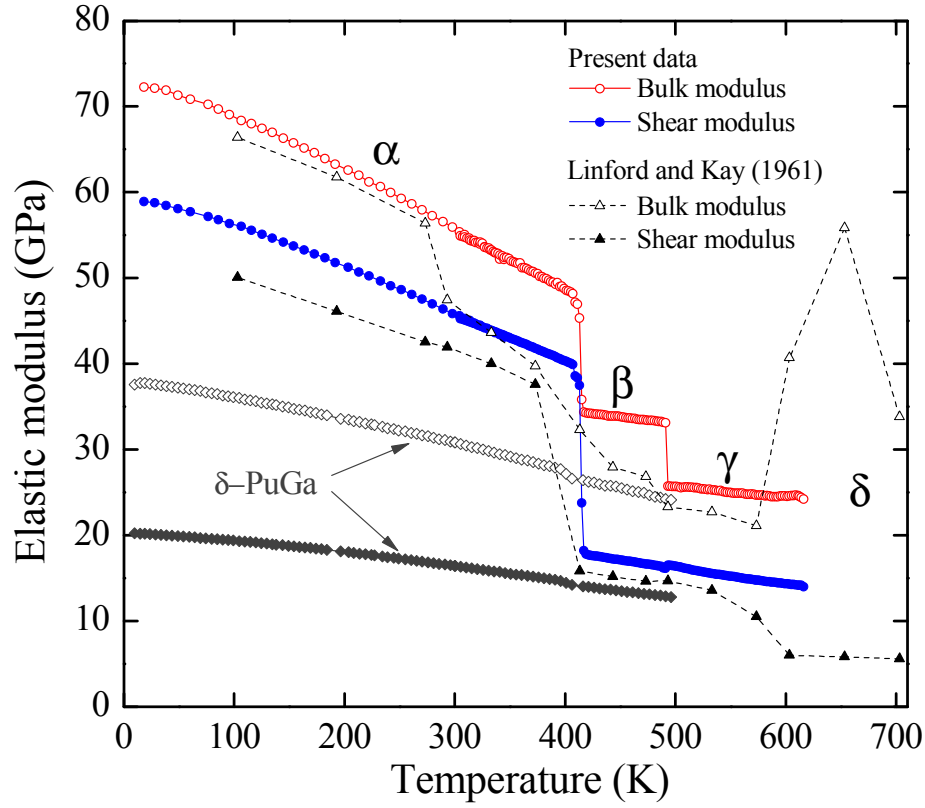
**Figure 2.** Bulk and shear moduli of pure Pu from 18 K to 616 K for α-Pu, β-Pu and γ-Pu compared to Linford and Kay[52]. The bulk moduli (empty diamonds) and shear moduli (solid diamonds) for δ-Pu 2.36 at. % Ga (previous work), are also plotted and are consistent with the values of pure Pu because the extrapolated values of δ-Pu 2.36 at. % Ga into pure γ-Pu's temperature range are smaller than that of γ-Pu as expected.
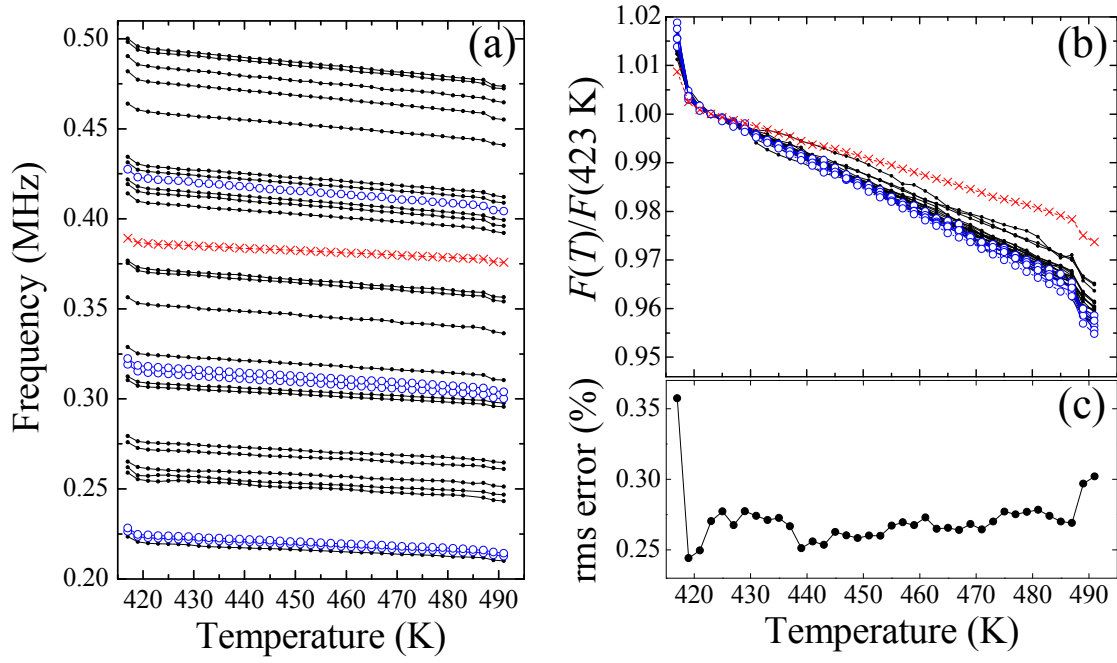
**Figure 3.** The temperature dependences of 28 resonances, which were used for the RUS fit for β-Pu, are plotted in (a). They are smooth and almost linear except at the phase boundaries. The RUS fit determined that the resonances in circles (○) in (a) and (b) are associated almost solely with the shear modulus, *G*, while crosses (×) are partially dependent on the longitudinal modulus, $C_L$. The ones in black depend on linear combinations of *G* and $C_L$. The frequencies in (a) were divided by the values at 423 K and are plotted in (c). This clearly shows the difference in the temperature dependences for the two modes. In (c), the rms % errors for 28 resonances are plotted. They are very small, less than 0.3 % and a little larger at the edges of the β phase.
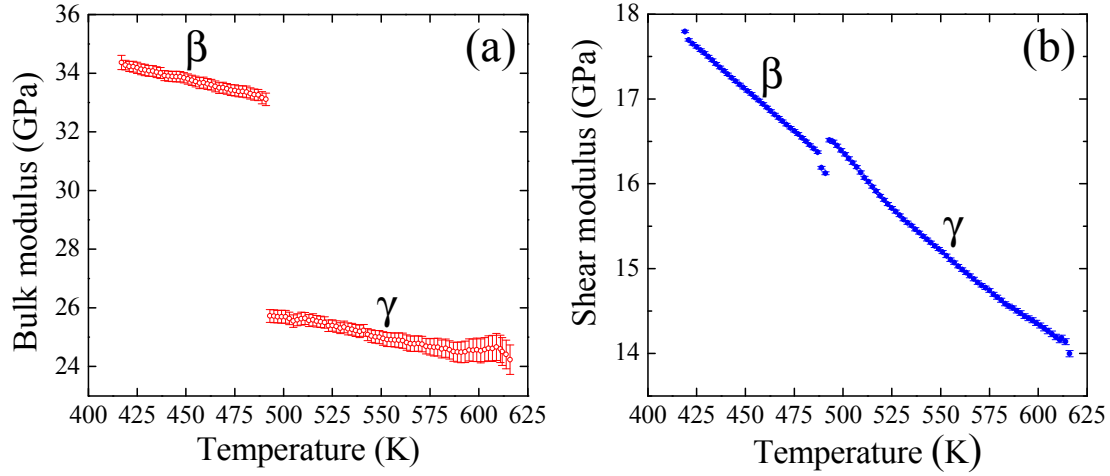
**Figure 4.** The bulk and shear moduli for β-Pu and γ-Pu are plotted in (a) and (b). The error bars represent the uncertainty which was produced by the inverse RUS calculation. The bulk modulus has larger error bars because few of the measured modes depend strongly on it. The non-monotonic behavior of the bulk modulus for γ-Pu at high temperature is probably an artifact of the RUS fit. A monotonic dependence is within the error bars. The bulk modulus has a clear jump at the β–γ transition. The shear modulus is similar between β-Pu and γ-Pu. This is surprising for a temperature-driven phase transition because shear phonon softening is often the primarily entropic driver of high temperature phase transitions.[86] The bulk modulus, which contributes less to lattice entropy, has a large decrease at the β–γ transition as expected, overwhelming the anomalous behavior of the shear modulus. The lattice entropy also depends on the atomic density which is reduced by 3% at the β–γ transition. Nevertheless, the calculated Debye temperature of γ-Pu is slightly larger than β-Pu. While this calculation is just a crude estimate, β-Pu and γ-Pu are closely competing phases in entropy and energy.[28, 40]
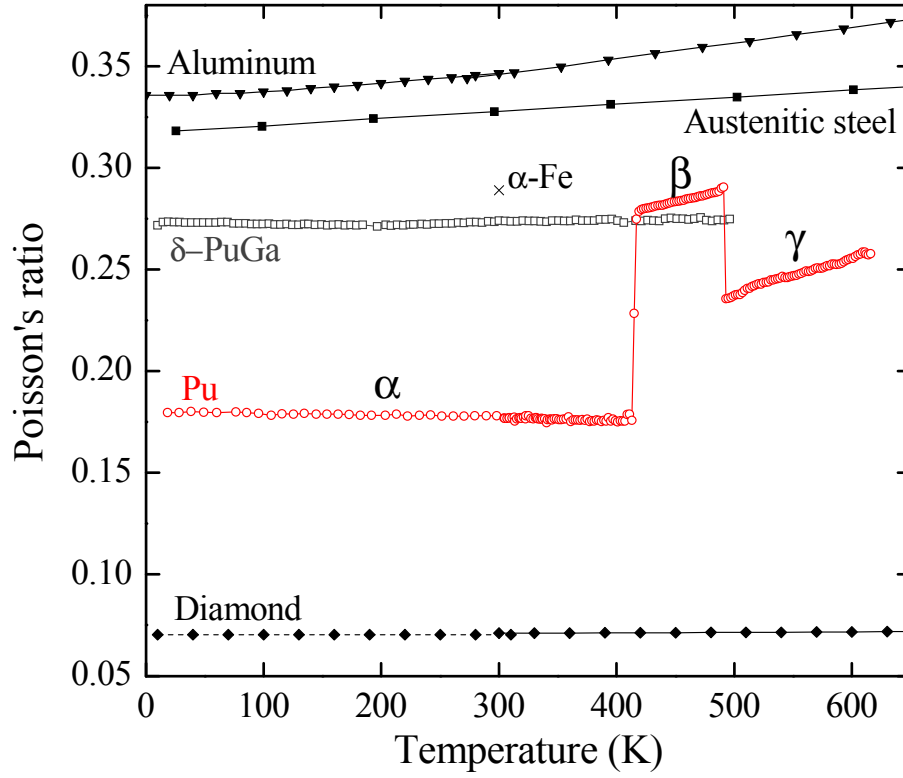
**Figure 5.** Poisson's ratio calculated from measured bulk and shear moduli is plotted. Poission's ratio for δ-Pu 2.36 at. % Ga is also plotted. The Poisson's ratios of aluminum[91, 92], austenitic steel[93], α-Fe[94] and diamond[95, 96] are plotted for comparison.[97] α-Pu, β-Pu and γ-Pu (and δ-Pu 2.36 at. % Ga) have large differences in their Poisson's ratios and temperature dependences as if they are completely different metals.